American Mineralogist, Volume 89, pages 211–218, 2004

Spiral growth of grossular under hydrothermal conditions

RALF MILKE[1,2,*]

[1]Universität Tübingen, Institut für Geowissenschaften, Wilhelmstrasse 56, 72074 Tübingen, Germany
[2]Geoforschungszentrum Potsdam, Department 4, Telegrafenberg, 14073 Potsdam, Germany

ABSTRACT

Grossular ($Grs_{99}Adr_{01}$) crystals were synthesized in hydrothermal experiments by the reaction wollastonite + calcite + anorthite = grossular + CO_2 (400 MPa; 695–750 °C; X_{CO_2} = 0.1; solid:fluid = 2:1) using natural minerals as starting materials. Growth spirals are visible due to silica decorations. The crystals are bounded by {110} and {211}. If crystallized at $T \leq 730$ °C, they are birefringent and show sector twinning; grown at $T \geq 730$ °C, they are optically isotropic. The crystal growth rates in the experiments ranged from about 1 to >100 μm/d. The edges of the growth terraces moved by 5–200 nm/s.

The morphology of the growth steps is interpreted against the background of supersaturation with respect to grossular in the fluid. The highest supersaturation occurs during the initial stage of the reaction (~1 h), ultimately at the wollastonite surfaces. In this initial stage, grossular crystallizes with only {111} faces present covered by round growth spirals. When a steady state with respect to dissolution and precipitation rates is reached (after ~24 h), all grossular crystals show {110} and {211} with polygonal spirals on {110} and parallel growth steps on {211}. All straight growth-step edges parallel [1$\bar{1}$1]. When the solid phases assume equilibrium with the fluid (after calcite in calcite-deficient experiments is used up completely), round growth spirals appear on {211}. The spirals are elongated parallel to [1$\bar{1}$1] and compete against parallel steps in that same direction. The surface morphology of the crystals synthesized under steady state conditions mimicks that of natural grandite crystals, and their growth rates equal the estimated growth rates of grandite crystals from natural hydrothermal systems.

INTRODUCTION

The surface of a growing crystal is bounded by interfaces with different atomic roughnesses. The normal growth rates of faces may be assumed qualitatively as being proportional to the degree of interface roughness. The rougher an interface, the larger is its normal growth rate such that the smoothest interface eventually remains as the habit-controlling face (Sunagawa 1987a). The surface topography of crystal faces can reveal growth mechanisms. At high supersaturation, the faces are generally rough and continuous growth occurs. As supersaturation decreases, the growth mechanism turns into layer growth by two-dimensional nucleation or at even lower supersaturation into spiral growth (Bennema et al. 1999).

This study has focused on exceptionally well-evolved growth spirals that have been observed on grossular-rich grandite crystals synthesized in hydrothermal experiments by the reaction calcite + wollastonite + anorthite = grossular + CO_2 using natural minerals. Part of the crystals formed in calcite-absent experiments by the reaction 2 Wo + 1 An = 1 Grs + 1 SiO_2, which occurs to a limited extent due to incongruent dissolution of wollastonite (Milke and Metz 2002). The surface morphology of the crystals is visible by scanning electron microscopy (SEM) due to preferential precipitation of quench SiO_2 on the growth-step edges. The observations are relevant to all growth-related aspects of grandites, such as crystal and surface morphology (Akizuki 1989; Jamtveit and Andersen 1992; Pearce 2001), birefringence (Hariya and Kimura 1978; Akizuki 1984; Allen and Buseck 1988), and oscillatory zoning (Jamtveit et al. 1995; Holten et al. 1997; Ivanova et al. 1998; Jamtveit 1999; Pollok et al. 2001).

Empirical knowledge has long established that the most common crystal form of natural grandite is the dodecahedron {110}, followed by the trapezohedron {211} (Pabst 1943). According to periodic bond chain (PBC) analyses and the Hartman-Perdok roughening theory (Hartman and Perdok 1955; Hartman and Bennema 1980; Bennema et al. 1999), both forms represent flat (F-)faces that may evolve by lateral spreading of growth spirals (Bennema et al. 1983). This morphology is consistent with kinetic models of garnet growth that consistently predict that, in grossular, {110} is morphologically most important followed by {211} (Cherepanova et al. 1992a, 1992b). On {110} of natural grandite crystals, rhombic growth hillocks have been observed in many cases, indicating that the faces grew by propagation of polygonal growth spirals (Isogami 1976; Akizuki 1989). The widespread rhombic step patterns on {110} faces of grandites also have been interpreted as spiral growth features (Jamtveit and Andersen 1992). In contrast to {110}, however, no growth spirals have so far been reported from {211} of grandite crystals. In spite of spiral patterns, {211} of grandites typically is striated parallel to the edges with {110} (e.g., Jamtveit and Andersen 1992; and our own observations on grandites from

* Present address: Universität Basel, Mineralogisch-Petrographisches Institut, Benoulli st., 30, 4051 Basel, Switzerland. E-mail: ralf.milke@unibas.ch

various locations). Transitions in crystal morphology have been observed on oscillatory zoned grandite crystals from the Oslo Rift, Norway, that went from planar via cellular to hopper-like growth (Jamtveit and Andersen 1992). During planar growth, dodecahedral faces {110} dominated, whereas during cellular and hopper growth, the ikositetrahedron {211} evolved. The morphological transitions are associated with the alternating flip-over between andradite-rich and andradite-poor compositions (Jamtveit 1999). This oscillatory zoning was ascribed to fluctuations in supersaturation, which might have originated from external (boiling, fluid mixing, temperature, and pressure fluctuations) or internal factors, resulting from self-organization in the interplay of fluid convection and crystal growth in the near vicinity of the growing crystals (Jamtveit et al. 1995; Holten et al. 1997; Pollok et al. 2001).

Very similar to grandites, pyralspite garnets also typically show polygonal hillocks on {110} together with striations on {211} (Isogami 1976). In the literature, there is only one example of spiral-type growth layers on {211} reported from pyralspite crystals, found on spessartine in the druses of rhyolithic lava at Wada-toge Pass, Japan (Endo and Sunagawa 1968). In contrast to natural garnets, beautiful growth spirals are known from both {110} and {211} of the synthetic garnets (YIG and YAG) grown from lead-oxide fluoride flux (Lefever and Chase 1962).

In this work, growth spirals on {211} of grandite crystals are described for the first time. The relationship between spirals on {110} and {211}, their occurence and morphology depending on surface supersaturation, and the significance of the observations for natural grandite crystallization, are discussed.

Experimental procedure

Sample description and treatment

Grossular-rich grandite was synthesized from a mixture of powdered natural wollastonite + calcite + anorthite in the presence of an H_2O-CO_2 fluid. The anorthite was from Miyakejima, Japan. In addition to the major elements it contains (in wt%) 0.48 FeO, 0.47 Na_2O, 0.21 MgO, 0.06 SrO, and 0.05 K_2O. The wollastonite was from Willsboro, NY, and contains (again in wt%) 0.39 FeO, 0.04 TiO_2, 0.02 K_2O, and 0.01 Na_2O, and 0.01 Al_2O_3. The calcite was clear Iceland spar and contains 0.07 wt% MnO. All reactants were powdered, hand-picked, and sieved to 80–100 µm. The initial X_{CO_2} was 0.10 and increased slightly during reaction due to the produced CO_2.

In most runs, the reactant mixtures were combined in stoichiometric proportions in terms of the reaction 1 Wo + 1 Cal + 1 An = 1 Grs + 1 CO_2. Several runs were performed without calcite or only with a strongly deficient amount with respect to the stoichiometric proportions. The reactant mixtures were sealed into Au capsules (20 mm long × 3 mm wide), together with H_2O and Ag oxalate. After welding, the capsules were stored for several hours at 110 °C to make sure that the Ag oxalate decomposed to Ag + CO_2 before the start of the runs. The amount of solid reactants per capsule was about 25 mg, and the amount of fluid about 12.5 mg.

All runs were carried out isobarically in conventional cold-seal pressure vessels at 400 MPa and temperatures between 665 and 750 °C, i.e., 10 to 85 °C above the equilibrium temperature as calculated with the data base of Gottschalk (1997). The isobaric heating took 30 min to reach run temperature. The run duration was between 1 and 240 h, and the conversion to grossular + CO_2 ranged from <1% to 30%. For more details, see Milke and Metz (2002).

Decoration of surface structures

The edges of growth layers are visible using SEM due to their decoration by silica that evolved during the isobaric quenching with compressed air. At 400 MPa, wollastonite is stable in contact with an aqueous fluid having X_{CO_2} = 0.1 at temperatures above 640 °C. It may be quenched without carbonation if a fast water-cooling method is used. Using compressed air, the quenching must be non-isobaric involving a pressure release during cooling such that the stability field of wollastonite is increased to lower temperatures. During a conventional isobaric cooling with compressed air, however, 5–10% of the wollastonite reacted with the fluid ($CaSiO_3 + CO_2 = CaCO_3 + SiO_2$). The quench-calcite crystallizes in situ on the wollastonite grains, whereas a large fraction of the produced SiO_2 instantly dissolves in the fluid and, during subsequent cooling, precipitates on high-energy sites at the grossular surfaces (like growth steps and crystal edges).

On the grossular crystals, this decoration is selective with respect to the crystal faces and edges. Silica precipitation is much more extensive on {110} than on {211} faces. In many cases, the [102] edges that point toward the fourfold axes [100] are decorated whereas the [131] edges that point toward the threefold axes [111] remain free (Fig. 1a). On most garnet faces, only irregularly scattered silica spherules are present or no decoration at all. Where spirals are incompletely decorated, the spiral steps are invisible by SEM (Fig. 1b). The apparent absence of spiral patterns on most crystals therefore does not mean that their faces are free from spiral steps.

Results

Observations on crystal morphology and optical birefrigence presented here include results on grossular crystals from the experiments of Milke and Metz (2002) that were synthesized in about 50 runs at temperatures from 665 to 750 °C, (durations of 1 to 1826 h) at a pressure of 400 MPa, with initial X_{CO_2} = 0.10. Under the conditions of the experiments, the fluid volume was about twice the volume of the solid minerals (Milke and Metz 2002) such that the grains were completely surrounded by the fluid. The garnet crystals grew into the fluid-filled voids of the loosely packed reactant mixture. After the runs, the mixture came out as a loose powder. Observations on spiral morphology are from several experiments that were terminated by isobaric quenching with compressed air (Table 1).

Chemical composition and zoning

The grandite crystals always contain minor amounts of the andradite component introduced by the natural minerals used as starting substances. Other elements present in the reactant minerals such as Ti, Mn, or Mg are not present in the garnet in concentrations above the detection limit of the microprobe. The andradite component is enriched in the crystal cores where Fe_2O_3 reaches up to 8 wt% ($Grs_{76}Adr_{24}$) or even more, as the strongly Fe-enriched core regions might be smaller than the spot size of the microprobe (Milke and Metz 2002). Outward from the cores the garnets have a uniform composition of $Grs_{99}Adr_{01}$. No complex or oscillatory zoning was observed. The decorated

Table 1. List of experiments and run conditions for experiments with growth step decoration on grandite crystals (except those noted)

Run no.	*T* (°C)	*t* (h)	Proportion of calcite*
WCAG 1	710	332	1
WCAG 2	750	332	1
WCAG 3	710	240	1
WCAG 4	695	240	1
WCAG 5	710	240	1
WCAG 6	695	240	1
WCAG 8	730	120	1
WCAG 9	700	120	0.1
G11†	745	1	1
G136	740	1	1
WA1	700	120	–
WA2[1]	700	120	–
WA3	710	120	–

* In fractions of the stoichiometric amount with respect to wollastonite + anorthite; stoich. amount = 1.
† Blow quench; no surface decorations.

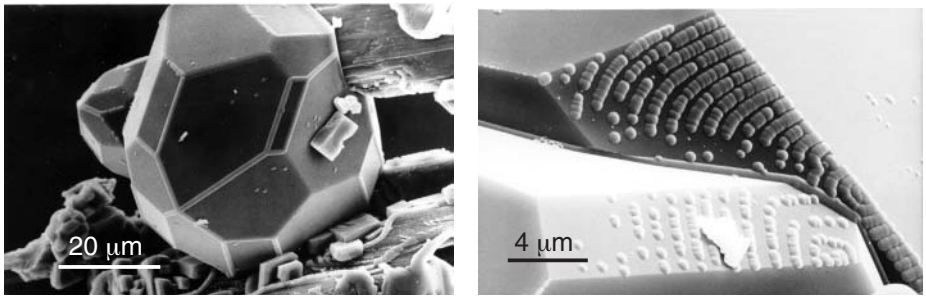

FIGURE 1. (a) Grossular overgrowing wollastonite with crystal-edge decorations. Silica decorates the edges parallel to [102] and [$1\bar{1}1$] whereas the edges parallel to [131] are uncoated. Quench calcite rhombohedra on the wollastonite surface. Run WCAG1, 710 °C, 332 h. **(b)** Incomplete spiral decoration on two adjacent {110} faces. Step width 500 nm. The surface steps are invisible where they are not decorated by silica spherules. Run WCAG6, 695 °C, 240 h.

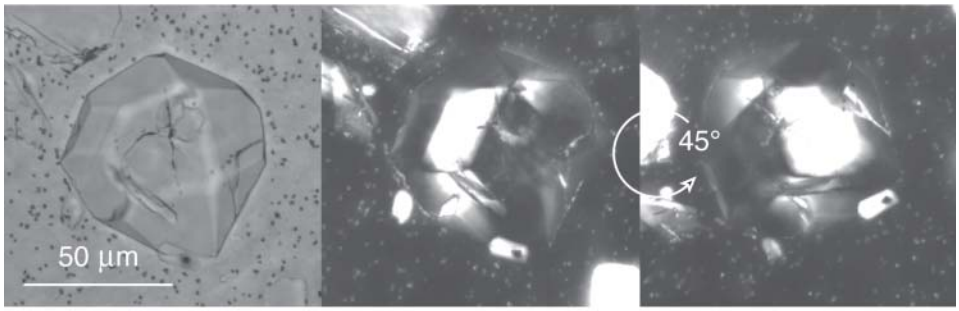

FIGURE 2. Large grossular crystal (70 μm diameter) embedded in epoxy with {211} dominating over {110}. Run G18 (Milke and Metz 2002), 675 °C, 621 h. Left picture in transmitted light, middle picture with crossed polarizers, right picture with crossed polarizers and turned 45°.

surfaces belong to crystals of about 10 μm diameter or more and are thus formed by Fe-poor grandite.

Optical anisotropy

The presence of optical anisotropy is a function of the growth temperatures. The grandite crystals grown at 710 °C or below are generally birefringent. Viewed under crossed polars, the crystals display sharp sector zoning if they are sufficiently large (Fig. 2). In very small crystals sector zoning is only vaguely visible. The zoning corresponds to sector-twinned crystals with four growth sectors under each dodecahedral face and vertices meeting at the center (Allen and Buseck 1988). At a growth temperature of 730 °C, only some of the crystals are birefringent whereas at 750 °C, all crystals are isotropic.

Crystal morphology

The morphology of the grandite crystals is simple and of little variability. No forms apart from {110} and {211} have been observed. During the initial stage of the experiments grandite crystallizes as pure dodecahedra. After 1 hour run time (runs G11 and G136), {110} is the only form present. After experiments lasting 24 h or longer, the crystals always are combinations of {110} and {211}. Thus, {211} faces evolve on the purely dodecahedral crystals during their subsequent growth. Crystals that nucleated later in the runs already start growing as combinations of {110} + {211}. In experiments with the stoichiometric starting mixture, the morphological importance of {110} mostly equals that of {211}, or {211} is slightly dominating. In experiments with little or no calcite in the starting mixture, {211} is by far the predominant form, but all crystals still show {110} faces. There is no systematic correlation between crystal habit and growth temperature or between habit and size.

Spiral morphology on {110}

During the initial stage of the experiments (runs G11 and G136), the spirals are almost perfectly round (Fig. 3a). The spiral steps are between 100 and 150 nm wide. The step widths are sometimes uniform over the entire faces, but in many cases they are rather alternating, suggesting that the steps comprise paired spirals consisting of two half steps. On the crystals showing both {110} and {211}, spiral and growth step decorations are almost totally restricted to {110}. The spirals are polygonalized with their arms parallel to the face edges, i.e., they always follow [$1\bar{1}1$]. The spirals commonly show interlaced step patterns. The step widths range from 250 to 700 nm, except for rare examples with wider growth terraces. Figure 3b shows a spiral on {110} that is also unusual in showing outward increasing step separations. The terrace width increases from 800 nm in the spiral center to 1600 nm in the margin. As the spiral center is located on a crystal edge, the increase in step width indicates an increase in surface supersaturation from the spiral center to the opposite edge (Sunagawa and Bennema 1982; Sunagawa 1987b). Both spirals seen on this crystal show interlaced step patterns (Bennema et al. 1983). Interestingly, due to the increase in step width most of the advancing upper half-layers do not catch up with the lower half-layers. Where more than one spiral center is present on one face, interaction and cooperation of neighboring spirals (Sunagawa and Bennema 1982) is commonly observed.

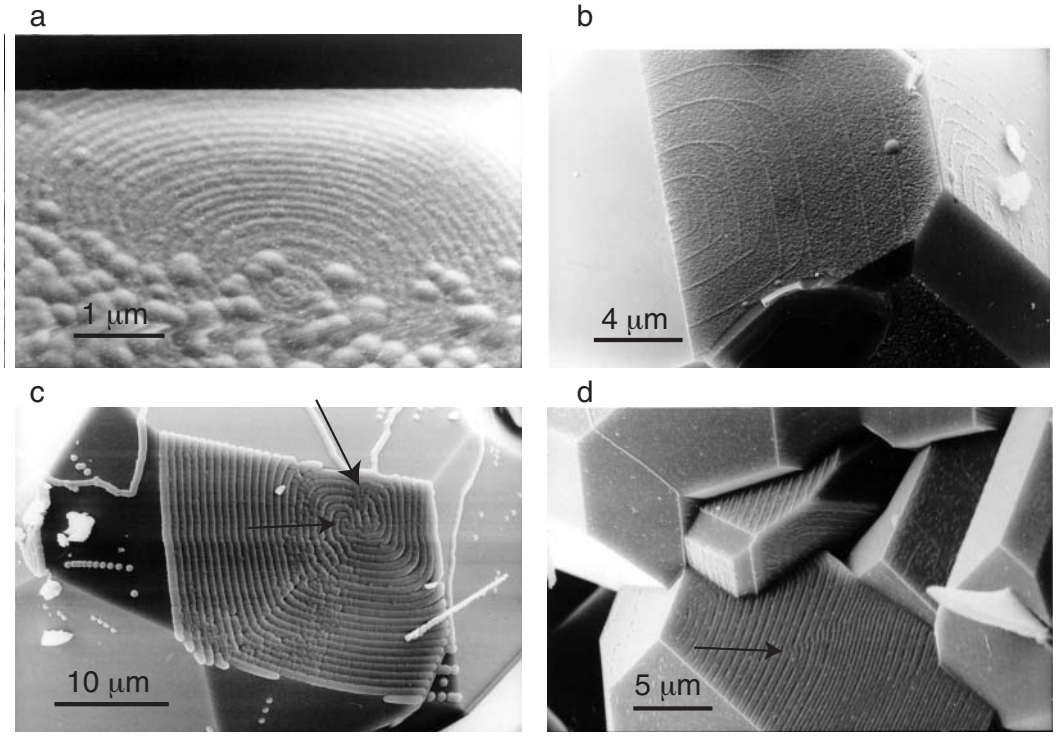

FIGURE 3. Step patterns on {110} (**a**) Round growth spiral that entirely covers a face of a purely dodecahedral crystal grown on wollastonite during the initial stage of the experiment G136 (740 °C, 1 h). (**b**) Spiral on {110} showing straight steps parallel to [1$\bar{1}$1] with unusually wide step separation extending from 800 nm in the spiral center to 1600 nm in the margin. Both spirals seen on this crystal show interlaced step patterns. Due to the increase in step width on the front face, most of the advancing upper half-layers do not catch up with the lower half-layers. Run WCAG6, 695 °C, 240 h. (**c**) Interaction of two spirals with opposite signs (arrows). After a few turns, both spirals form a single system of polygonal steps. In the center of the spiral system, several steps are cut to allow the two spirals to merge into one. WCAG6, 695 °C, 240 h. (**d**) A large face covered by paired polygonal spiral steps (average step width 270 nm) emerging from a dislocation near the edge and dominating a second spiral center (arrow). The spirals on {110} of the adjacent crystals have a step width of 540 nm. WCAG5, 710 °C, 240 h.

The interaction of two spirals with opposite signs is seen on Figure 3c. After a few turns, the two spirals merge into a single system of polygonal steps. Perturbations occur where the two step systems do not fit. Figure 3d shows a paired polygonal spiral (average step width 270 nm) that emerges from a dislocation near the edge and extends over the entire face, thereby dominating a spiral in the center. The spirals on {110} of the adjacent crystals have a step width of 540 nm. Because it appears improbable that the surface supersaturation is different for these neighboring and equivalent faces, it is possible that the wider steps represent closely paired double steps.

Spiral morphology on {211}

On most crystals from stoichiometric experiments, {211} faces are not decorated at all or only covered by irregularly scattered silica spherules. Only in rare cases, there are weak decorations parallel to [1$\bar{1}$1] with step spacings around 600 nm (Fig. 4a). Exceptional crystals were found in one experiment overgrowing the silver precipitate that had formed due to the breakdown of Ag oxalate in one end of the sample tube (Fig 4b). These are the only crystals from stoichiometric experiments that show a distinct decoration of step patterns on {211}. Steps (sub-)parallel to [1$\bar{1}$1] occur together with elongated spirals. The spirals transform into parallel steps where their round ends reach the face edges. Spacings between the (sub-)parallel growth steps are between 300 and 500 nm and are about doubled in the curved parts of the spirals and the wavy parts of the step patterns, thus indicating faster step propagation along the rougher portions of the steps. Complex patterns result from the interaction of parallel step systems with spiral centers.

Grandite crystals from experiments without or with only small fractions of calcite in the starting mixtures (WCAG 9, WA1, WA2, WA3) are always combinations of {110} + {211} with {211} dominating. The {211} faces bear round and often slightly elongated, very well-decorated step patterns. Growth terraces on adjacent faces do not correlate, thus indicating an independent evolution of each single face (Fig. 4c). With increasing distance from the spiral centers, the curvature of the growth steps decreases, so that they gradually transform into step systems sub-parallel to [1$\bar{1}$1] (Fig. 4d). Most faces are dominated by one single spiral system. Figure 4d shows a line of spiral centers possibly representing a screw boundary that are dominated by a single spiral system. Single and paired spirals occur with similar morphology (Fig. 4e). Where two large spirals are present on one face they tend to merge into a combined step system due to the reentrant-corner effect, i.e., the faster advance of reentrant corners due to their larger supply of crystallizing entities (Sunagawa and Bennema 1982) (Fig. 4f). The {110} faces on these

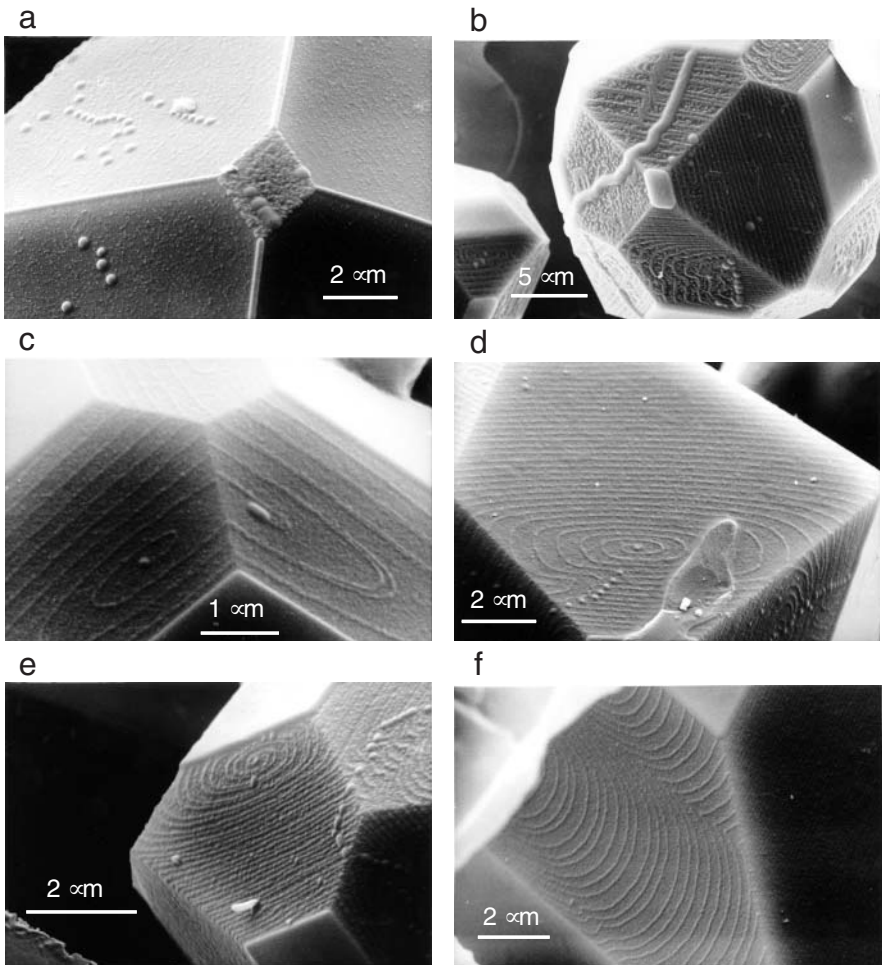

FIGURE 4. Step patterns on {211} (**a**) View on {110} of a grossular crystal from the stoichiometric run WCAG3 with dense silica coating but no visible spiral pattern. The crystal grew inside the reactant mixture. Thin decoration of steps on the four {211} faces are parallel [1$\bar{1}$1]. WCAG3, 710°C, 240 h. (**b**) Grossular from the Ag precipitate in a remote end of the sample tube of run WCAG3. Growth on {211} by competition of growth steps parallel to [1$\bar{1}$1] emerging from the edges with {110} and elongated growth spirals. Thick silica caps on {110} hide all surface structures. 710 °C, 240 h. (**c**) View on three {211} faces around [111] of a 12 µm large crystal from experiment WA1 without any calcite in the starting mixture. One single system of round growth spirals on each face. The spiral systems on adjacent faces share no step positions and obviously are independent from each other. 700 °C, 120 h. (**d**) {211} face covered by one single spiral system. The line of dominated spiral centers in the lower left of the picture probably represents a screw boundary. The dominant spiral is elongated parallel to the edge with {110} (= parallel to the upper picture margin). Its roundness decreases with increasing distance from the spiral center. At the same time, step spacings decrease as is best seen at the edge of the face. Run WCAG9, 700 °C, 120 h, calcite strongly deficient in the starting mixture. (**e**) Detail from a large grossular crystal (25 µm diameter) from the strongly calcite-deficient run WCAG9. All {110} faces are covered by a thick silica coating; spiral decorations appear on all {211} faces. This face is made up of a round paired spiral that is elongated parallel to the edge with {110} and gradually evolves into edge-parallel steps. 700 °C, 120 h. (**f**) (211) face with two large spiral systems that both emerge from centers on the egde of the face. The angle between the growth steps continously decreases due to the reentrant corner effect. In the lower part of the picture, a small reentrant corner probably emerges from a dominated spiral center and is obliterated after only a few spiral turns by the same effect. WCAG9, 700 °C, 120 h.

crystals are always covered by a thick silica cap that hides any surface topography.

DISCUSSION

Birefrigence

Several hypotheses have been proposed for the origin of birefringence in grandites, such as: (1) ordering of Fe^{3+} and Al on octahedral sites (Takéuchi et al. 1982; Akizuki 1984; Allen and Buseck 1988; Kingma and Downs 1989); (2) noncubic incorporation of OH-groups (Rossman and Aines 1986; Allen and Buseck 1988); and (3) strain from compositional boundaries (Lessing and Standish 1973; Kitamura and Komatsu 1978; Pollok et al. 2001). The sector zoning of the synthetic crystals under crossed polars matches the models suggested by Akizuki (1984) and Allen and Buseck (1988) assuming Fe^{3+}-Al-ordering on the octahedral sites. If Fe^{3+} and Al are ordered, this ordering must have occured during incorporation at the growth steps that correspond to the [1$\bar{1}$1]-steps of polygonal spirals on {110}. Apart from their more andradite-rich cores, the grandite crystals from the experiments contain only about 1 mol% andradite component. Iron concentrations as small as this apparently are responsible for the optical anisotropy of Eden Mills grossular (Allen and Buseck 1988). The Fe^{3+}-Al-ordering model was recently disputed by Becker and Pollock (2002) who concluded from Monte Carlo simulations that ordering in grandites is thermodynamically stable only at temperatures below ≈500 K for grandite with 1:1 ratio of Al and Fe^{3+} and even less for near end-member compositions. Moreover, Pollock et al. (2001) pointed out that under metastable conditions, the kinetics tends to favor the growth of disordered rather than ordered structures. However, both the sector zoning and the correlation of optical anisotropy with growth temperature support the assumption that cation ordering is responsible for the birefringence. The transition from anisotropic to isotropic grandite in the experiments is only slightly higher than the temperatures reported by Hariya and Kimura (1978) for intermediate grandite compositions (Fig.

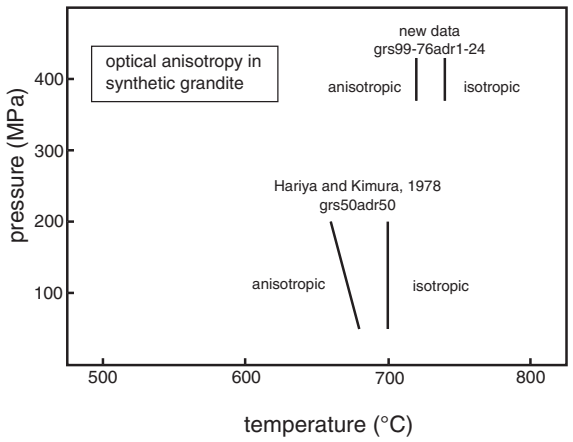

FIGURE 5. Transition from optically anisotropic to isotropic grandite in the growth and heating experiments of Hariya and Kimura (1978) and the experiments presented here. Despite the different solid solution compositions, the transition temperature is similar.

5). By compiling results from crystallization and equilibration experiments for $Grs_{50}Adr_{50}$ grandite, they found a transition from anisotropic to isotropic grandite at temperatures slightly below 700 °C, with a tendency to lower temperatures at higher pressure. The new growth experiments with andradite-poor composition at higher pressure indicate a similar transition temperature. The ordering process responsible for the birefringence in intermediate and grossular-rich synthetic grandite thus seems to be largely controlled by the growth temperature, whereas chemical composition, growth medium, and pressure are only minor factors.

Step height

The step height can be assessed only indirectly because the actual steps are not seen but only their decorations. However, inferring from the commonly observed interlaced patterns, it is probable that most growth layers are monomolecular. Interlaced patterns on {110} of garnet are explained by splitting of a 9 Å high growth layer into two half-layers of 4.5 Å (Bennema et al. 1983). Applying a width:height relation of 100:1000, as is typically observed on crystals grown from aqueous solutions (Sunagawa 1978), 9 Å thick growth layers would correspond to 90 to 900 nm wide spiral terraces, which very well match the observed range.

Crystal and surface morphology related to supersaturation

The observed variations in morphology and step patterns are interpreted against the background of supersaturation. Although it is not possible to quantify the activities of dissolved species in the H_2O-CO_2 fluid or the surface supersaturation of the growing grandite crystals, it is possible to define a sequence from relatively high supersaturation to near-equilibrium conditions, depending on the setup and duration of the experiments. The activities of dissolved species during a heterogeneous reaction in a closed sample tube evolve by the interplay of dissolution and precipitation rates (Lüttge and Metz 1991). The activities of dissolved species increase in the early stage of the experiments due to dissolution of the reactants (calcite, wollastonite, and anorthite in the present case). When the nucleation barrier is exceeded, nucleation and growth of the product phase (grossular) sets in. After going through a maximum, the activities in the fluid level off in a steady state between dissolution and precipitation rates that holds until one of the reactants is consumed. The reaction then ceases and the fluid phase assumes equilibrium with the products and persisting reactants. In the present reaction, the timing and duration of these stages was monitored at 730 °C by measuring grandite nucleation and growth rates (Milke and Metz 2002). Already during the first hour of the experiments, the nucleation barrier for grandite on the surfaces of the wollastonite grains is exceeded locally. On the scale of the entire sample tubes, the nucleation rate maximum is reached during the second day, and a steady state is reached during the third day of the experiments. In the runs with very little calcite in the starting mixture, the fluid assumes equilibrium with anorthite, wollastonite, and grossular when calcite is consumed. When no calcite is present, still a small amount of grossular crystallizes due to the well-known incongruent dissolution of wollastonite resulting from the initially fast leaching of Ca from its surface layer (Casey et al. 1993). This effect results in an initially high supersaturation with respect to grandite on the wollastonite surfaces (Milke and Metz 2002). Supersaturation becomes manifest in the very high initial growth rates leading to crystals 10 µm in size after only one h run duration. The grossular crystals on wollastonite at the very beginning of the experiments thus represent the highest degree of supersaturation. The crystals from the steady state stage of the experiments grew under medium supersaturation, and those from the calcite-deficient experiments represent the approaching of equilibrium conditions. Table 2 shows how the relative normal growth rates in [110] and [211] direction as well as growth step and spiral morphology evolve relative to supersaturation. At high supersaturation, the normal growth rates of {211} are more than 1.15 times higher than normal to {110}, such that only {110} is present morphologically. At very low supersaturation, {211} dominates, although {110} is always there, i.e., growth in the [110] direction was less than 1.15 times faster than in [211] direction before the reaction ceased. The initially round growth spirals on {110} polygonalize with decreasing supersaturation and develop straight steps in the $[1\bar{1}1]$ direction. On {211}, round growth spirals only appear at low supersaturation and under near-equilibrium conditions. At higher supersaturation, they compete with growth steps parallel to $[1\bar{1}1]$ that emerge from the piling up of growth layers on {110}. During steady state crystallization, these parallel steps totally dominate the spiral growth centers on the {211} faces. It is likely that the faces grew largely by parallel step propagation, and that the spirals only evolved in the latest stages before the crystal growth dissipated.

The morphological observations are not always in accordance with predictions from the PBC theory (Bennema et al. 1999). Bennema et al. (1983) demonstrated that the theoretical morphology (MI) can be deduced from dimensionless edge energies, ε, for minimal energy edges in the PBC directions. The edge energy corresponds with the energy of the bonds in a slice d_{hkl} that are broken by the edge, and is complementary to the attachment energy. Calculated edge energies for slices relevant to crystals that show {110}+{211} are given in Table 3. For polygonal spiral growth, the theoretical MI of a face runs parallel to $\varepsilon_1 + \varepsilon_2$. For both crystallographic forms, there exist two F-slices labeled 1 and 2. According to Table, 3 for both

TABLE 2. Relative morphological importance of {110} and {211} step width and morphology on the respective faces for different stages of the experiments

Reaction stage	MI*	Steps on {110}		Steps on {211}	
		width [nm]	shape	width [nm]	shape
initial stage	only {110}	100–150	round spirals	–	–
steady state					
a)within reactant mixture	{211}≥{110}	250–700 (1600)	polygonal spirals	600	only parallel striation
b) remote position in sample tube	{211}>{110}	?	?	sub-parallel: 250–500 curved: 600–1000	parallel striation + elongated round spirals
near equilibrium	{211}>{110}	?	?	sub-parallel: 100–200 curved: 300–500	less elongated round spirals

TABLE 3. Dimensionless edge energies calculated after Bennema et al. (1983) for directions of minimal edge energies using the transformation formalism of Van der Eerden and Bennema (1983) and the ratio of bond energies based on Human et al. (1981)

F-slice	Directions	$\varepsilon_{1,2}$	$\varepsilon_1 + \varepsilon_2$
$(\bar{1}12)_1$	$[1\bar{1}1]$	3.41	9.27
	[110]	5.86	
$(\bar{1}12)_2$	$[1\bar{1}1]$	3.42	7.52
	[110]	4.10	
$(022)_1$	$[0\bar{1}1]$	6.82	15.13
	$[1\bar{1}1]$	8.31	
$(022)_2$	$[0\bar{1}1]$	2.28	5.19
	$[1\bar{1}1]$	2.91	

forms the slice labeled 1 should be dominant and {110} should be morphologically more important than {211}. It thus appears contradictory to theory that {211} is dominant when equilibrium conditions are approached.

The prominent role of the polygonalized spiral steps parallel to $[1\bar{1}1]$ on {110} is well in accordance with their high edge-energy value. Several observations correspond with general relations between growth spiral and crystal morphology (Sunagawa 1987a):

(1) the spirals on {110}, the form with the highest theoretical MI, are more polygonalized than those on {211}; (2) the spiral step separations are wider on {110} than on {211}; and (3) the spirals on {110} are rougher under higher supersaturation.

However, the edge-energy calculations do not explain the dominance of parallel steps over growth spirals on {211} except at near-equilibrium conditions. Similar observations have been made on other minerals, for example pyrite, which shows large habit-controlling faces that should not be the morphologically most important faces according to PBC analyses and that only show striations instead of growth spirals (Sunagawa 1987b). The dominance of parallel steps on {211} is reminiscent of the common occurence of habit-controlling {211} faces on natural grandites and other natural silicate garnets that never show growth spirals but only parallel steps of growth layers that pile up on {110} (Sunagawa 1987a). It appears that in these cases, the kinetics of step advancement on the individual faces play a key role in controlling the macromorphology.

Figures 4d and 4e demonstrate how the dominance of the parallel growth steps on grossular-rich grandite evolves. Due to the slower propagation of the edge-parallel steps, the growth spirals elongate in that same direction such that the curved portions of the steps tend to grow out of the faces. Along the edges, the roundness disappears from the steps as the distance from the spiral center increases. At the same time, the step spacings decrease, i.e., the propagation of the steps is slowed down (Figs. 4d and 4e). The step advance in $[0\bar{1}1]$ direction (normal to the edge) to $[1\bar{1}1]$ (edge-parallel) at near equilibrium conditions is about 1:2. On the crystals, overgrown on the Ag precipitate in the stoichiometric experiment G136, the ratio of edge-normal vs. edge-parallel advance is about 1:3 to 1:4. It thus seems that the discrepancy between edge-normal and edge-parallel step propagation increases with supersaturation. As a consequence, the spirals eliminate themselves under steady state conditions, and {211} only grows by steps that pile up on the {110} faces. This growth mechanism requires that the growth steps on {211} are polygonized such that the advancing steps are edge-parallel. Consequently, purely dodecahedral crystals only evolve under high supersaturation when the growth steps on {110} are rough and round.

Crystal growth rates and step advance rates

During steady state crystallization, the crystals grew by 1–3 μm/day (~0.1 μm/h). In the initial stage, the growth rates reached up to 10 μm/h. The largest crystals after 10-day experiments at 730 °C measured 50 μm, whereby 75% of their final diameters were already reached after the first 48 hours (Milke and Metz 2002). To form a 50 μm diameter crystal, 28000 monomolecular growth layers had to pile up on the {110} faces, 7000 of which (25% of the diameters) attached during the steady state crystallization from day 3 through 10. This attachement rate means that during steady state crystallization, one spiral turn occured every 100 seconds and that the parallel growth steps moved by 5 nm/s. During the first 48 h, the steps move much faster. Integrating over the first 48 h, the average time for one spiral turn is 8 s but actually one turn takes much less than 1 s during the initial stage of the runs. By forming almost 10 μm large crystals within 1 h run time, the round spiral steps must have moved by 100–200 nm/s, which comes up to the width of one growth terrace. From the initial through the steady state crystallization, the rate of spiral step advance thus decreased by a factor of 20–40. At the same time, the step density decreased by a factor of 5, such that a 100- or 200-fold decrease in normal growth rates resulted.

Fast crystal growth in geosystems is assumed to occur when hydrothermal solutions circulate through pores and fractures. A common feature in such environments is oscillatory zoning, which usually is associated with self-organization between surface reactions and diffusion in the surrounding fluid and thus requires high growth rates (Yardley et al. 1991). For the oszillatory zoned grandites in the Oslo Rift, Norway, Jamtveit et al.

(1995) considered growth rates ≥ 1 µm/day to be sufficiently fast to produce a significant depletion of Fe at the mineral-fluid interface, which is a precondition for the periodic switch-over of the garnet composition. Growth took place at temperatures of 350–400 °C and pressures of 200–300 bar (Jamtveit and Andersen 1992). In the experiments, there was only less than 0.5 wt% FeO present in the starting mixture, which explains the absence of oscillatory zoning. However, dissolution halos around the dodecahedral grossular crystals in the initial stage of the reaction indicate the existence of near-surface diffusion gradients (Milke and Metz 2002). Despite the much higher temperatures and pressure in the experiments, the measured growth rates equal the estimated growth rates from the Oslo Rift. This agreement is not a necessary consequence of the chosen run conditions. The experiments have only a certain *P*,*T*,*X*-window where grossular growth can be studied within hours to weeks. But even in this restricted range of reaction rates, there is large leeway concerning nucleation and growth rates. For example, the formation of 2.5 mg grossular (i.e., a run with 10% conversion) could as well be achieved by growth of one single crystal of 0.7 mm diameter or by 1.3×10^9 crystals of 1 µm diameter, spanning a range over 3 orders of magnitude for growth rates, and 9 orders of magnitude for nucleation rates. Moreover, the synthetic crystals from steady state crystallization and their natural counterparts bear analogous surface structures. Both show polygonal growth spirals on {110} and parallel striations on {211}. Given this close similarity in surface morphology, the coincidence of growth rates might not be accidental. It might rather reflect a virtually identical surface supersaturation evolving in the diffusion field between crystal surfaces and the fluid in either case and the strict surface control of this process.

ACKNOWLEDGMENTS

Part of the experiments were done during my Ph.D. thesis supervised by P. Metz at the University of Tübingen. I thank P. Bennema and B. Jamtveit for their careful reviews. Thanks for manifold technical assistence go to M. Hertel and to R. Hüttemann for the hours at the SEM. I. Sunagawa is thanked for his advice and literature on growth spirals.

REFERENCES CITED

Akizuki, M. (1984) Origin of optical variations in grossular-andradite garnet. American Mineralogist, 69, 328–338.

———(1989) Growth structure and crystal chemistry of grossular garnets from the Jeffrey Mine, Asbestos, Quebec, Canada. American Mineralogist, 74, 859–864.

Allen, F.M. and Buseck, P.R. (1988) XRD, FTIR, and TEM studies of optically anisotropic grossular garnets. American Mineralogist, 73, 568–584.

Becker, U. and Pollock, K. (2002) Molecular simulations of interfacial and thermodynamic mixing properties of grossular-andradite garnets. Physics and Chemistry of Minerals, 29, 52–64.

Bennema, P., Giess, E.A., and Weidenborner, J.E. (1983) Morphology of garnets and structure of F slices determined from a PBC analysis. Journal of Crystal Growth, 62, 41–60.

Bennema, P., Meekes, H., and Van Enckevort, W.J.P. (1999) Crystal growth and morphology: A multi-faceted approach. In Growth, Dissolution and Pattern Formation in Geosystems, B. Jamtveit and P. Meakin, Eds., p. 21–64. Kluwer Academic Publishers, Dordrecht, The Netherlands.

Casey, W.H., Westrich, H.R., Banfield, J.F., Ferruzzi, G., and Arnold, G.F. (1993) Leaching and reconstruction at the surfaces of dissolving chain-silicate minerals. Nature, 366, 253–256.

Cherepanova, T.A., Bennema, P., Yanson, Yu.A., and Tsukamoto, K. (1992a) Advance velocity of steps on {211} and {110} faces of yttrium iron garnet: theory and observations. Journal of Crystal Growth, 121, 1–16.

Cherepanova, T.A., Bennema, P., Yanson, Yu.A., and Vogels, L.J.P. (1992b) Morphology of synthetic and natural garnets: theory and observations. Journal of Crystal Growth, 121, 17–32.

Endo, Y. and Sunagawa, I. (1968) Structures of garnet from Wada-toge Pass, Nagano Prefecture. Journal of the Mineralogical Society of Japan, 9, 69–80 (in Japanese).

Gottschalk, M. (1997) Internally consistent thermodynamic data for rock forming minerals in system SiO_2-TiO_2-Al_2O_3-Fe_2O_3-CaO-MgO-FeOrK_2O-Na_2O-H_2O-CO_2. European Journal of Mineralogy, 9, 175–223.

Hariya, Y. and Kimura, M. (1978) Optical anomaly garnet and its stability field at high pressures and temperatures. Journal of the Faculty of Sciences, Hokkaido University, Series IV, 18, 611–624.

Hartman, P. and Bennema, P. (1980) The attachment energy as a habit controlling factor, 1. Theoretical considerations. Journal of Crystal Growth, 49, 145–156.

Hartman, P. and Perdok, W.G. (1955) On the relation between structure and morphology of crystals. Acta Crystallographica, 8, 49–52, 521–524, 525–529.

Holten, T., Jamtveit, B., Meakin, P., Cortini, M., Blundy, J., and Austrheim, H. (1997) Statistical characteristics and origin of oscillatory zoning in crystals. American Mineralogist, 82, 596–606.

Human, H.J., Van der Eerden, J.P., Jetten, L.A.M.J., and Odekerken, J.G.M. (1981) On the roughening transition of biphenyl: Transition of faceted to non-faceted growth of biphenyl for growth from different organic solvents and the melt. Journal of Crystal Growth, 51, 589–600.

Isogami, M. (1976) Morphology and optical anomaly of silicate garnets—An approach from elasticity theory. Thesis, Tohoku University, Tsukuba, Japan.

Ivanova, T.I., Shtukenberg, A.G., Punin, Y.O., Frank-Kamenetskaya, O.V., and Sokolov, P.B. (1998) On the complex zonality in grandite garnets and implications. Mineralogical Magazine, 62, 857–868.

Jamtveit, B. (1999) Crystal growth and intracrystalline zonation patterns in hydrothermal environments. In Growth, Dissolution and Pattern Formation in Geosystems, B. Jamtveit and P. Meakin Eds, p.65–84, Kluwer Academic Publishers, Dordrecht, The Netherlands.

Jamtveit, B. and Andersen, T.B. (1992) Morphological instabilities during rapid growth of metamorphic garnets. Physics and Chemistry of Minerals, 19, 176–184.

Jamtveit, B., Ragnarsdottir, K.V., and Wood, B.J. (1995) On the origin of zoned grossular-andradite garnets in hydrothermal systems. European Journal of Mineralogy, 7, 1399–1410.

Kingma, K.J. and Downs, J.W. (1989) Crystal-structure analysis of a birefringent andradite. American Mineralogist, 74, 1307–1316.

Kitamura, K. and Komatsu, H. (1978) Optical anisotropy associated with growth strain of yttrium garnet, $Y_3(Al, Fe)_5O_{12}$. Kristall und Technik, 13, 811–816.

Lefever, R.A.and Chase, A.B. (1962) Analysis of surface features on single crystals of synthetic garnets. Journal of the American Ceramic Society, 45, 32–36.

Lessing, P. and Standish, R.P. (1973) Zoned garnet from Crested Butte, Colorado. American Mineralogist, 58, 840–842.

Lüttge, A. and Metz, P. (1991) Mechanism and kinetics of the reaction 1 dolomite + 2 quartz = 1 diopside + 2 CO_2 investigated by powder experiments. Canadian Mineralogist, 29, 803–821.

Milke, R. and Metz, P. (2002) Experimental investigation of the kinetics of the reaction wollastonite + calcite + anorthite = grossular + CO_2. American Journal of Science, 302, 312–345.

Pabst, A. (1943) Large and small garnets from Fort Wrangell, Alaska. American Mineralogist, 28, 233–245.

Pearce, T.H. (2001) Pristine surface growth features on 100 Ma garnet phenocrysts: Interference imaging results. American Mineralogist, 86, 1302–1306.

Pollok, K., Jamtveit, B., and Putnis, A. (2001) Analytical transmission electron microscopy of oscillatory zoned grandite garnets. Contributions to Minealogy and Petrology, 141, 358–366.

Rossman, G.R. and Aines, R.D. (1986) Spectroscopy of a birefringent grossular from Asbestos, Quebec, Canada. American Mineralogist, 71, 779–780.

Sunagawa, I. (1978) Vapor growth and epitaxy of minerals and synthetic crystals. Journal of Crystal Growth, 45, 3–12.

———(1987a) Surface microtopography of crystal faces. In Morphology of Crystals. Part A, I. Sunagawa, Ed., p. 321–365. Terrapub, Tokyo.

———(1987b) Morphology of minerals. In Morphology of Crystals. Part B, I. Sunagawa, Ed., p. 511–587. Terrapub, Tokyo.

Sunagawa, I. and Bennema, P. (1982) Morphology of growth spirals: Theoretical and experimental. In W.R. Wilcox, Ed., Preparation and properties of solid state materials, Vol. 7, 1–129. Growth mechanisms and silicon nitride, Dekker, New York.

Takéuchi, Y., Haga, N., Shigemoto, U., and Sato, G. (1982) The derivative structure of silicate garnets in grandite. Zeitschrift für Kristallographie, 158, 53–99.

Van der Eerden, J.P. and Bennema, P. (1983) Star-tetrahedron transformation and calculation of bond energies at the crystal-mother phase boundary. Journal of Crystal Growth, 61, 45–52.

Yardley, B.W.D., Rochelle, C.A., Barnicoat, A.C., and Lloyd, G.E. (1991) Oscillatory zoning in metamorphic minerals: an indicator of infiltration metasomatism. Mineralogical Magazine, 55, 357–365.

MANUSCRIPT RECEIVED JUNE 2, 2003
MANUSCRIPT ACCEPTED SEPTEMBER 18, 2003
MANUSCRIPT HANDLED BY KEVIN ROSSO